PAPER

CrossMark
← click for updates

Surface modification by physical treatments on biomedical grade metals to improve adhesion for bonding hybrid non-isocyanate urethanes

K. M. F. Rossi de Aguiar,[*a] U. Specht,[b] J. F. Maass,[c] D. Salz,[b] C. A. Picon,[d] P.-L. M. Noeske,[b] K. Rischka[b] and U. P. Rodrigues-Filho[a]

This work aims to improve the adhesion of a hybrid non-isocyanate polydimethylsiloxane urethane (PDMSUr) coating by producing active layers on titanium alloy (Ti6Al4V) and stainless steel (SS316L) applying pulsed Nd:YAG laser and oxygen plasma. The PDMSUr is a hybrid adhesive and, when functionalized with alkoxysilane groups, can bind onto the interfacial hydroxyl groups of a (hydr)oxide/carbonate layer by sol–gel reactions. These reactions are acid catalysed and the silanol groups can bind through Si−O−metal links. The pull-off-strength of such sustainable coatings raised more than 100% for both substrates after the physical treatments, compared with the substrates etched. X-ray Photoelectron Spectroscopy (XPS) of a freshly pre-treated substrate revealed the formation of thin oxide-based reactive layers on the surface of Ti6Al4V and SS316L after the surface treatments. Both physical procedures were efficient to create oxide layers on top of metallic substrates and contributed to the improvement of adhesion strength of PDMSUr on biomedical grade metals.

Introduction

Stainless steel (SS316L), titanium and its alloys are the most widely used biomedical grade materials for dental braces, wires and implants.[1,2] Biocompatibility, low toxicity and low corrosion rates[3] of titanium alloys are widely known as its main characteristics, as well as strength and low Young's modulus.[4,5] Both bare SS316L and titanium alloy surfaces obtained in air are often covered by a native oxide layer terminated by hydroxyl and carbonate species. In this state, some uniform corrosion resistance is observed; however, reliably avoiding localized breakdown[6] or crevice corrosion is challenging when applying these materials in implants. In this case, after corrosion and surface film dissolution some toxic ions, such as vanadium or nickel[7] can be released, which are not biocompatible with the human body.[8] The accumulation of these toxic metallic ions can result in adverse biological reactions, cytotoxicity, inflammatory reactions and, genotoxicity[3] besides leading to mechanical failure of the implanted device.[9] An alternative to avoid corrosion or other damages on the metallic surface is coating it with

an appropriate material, *e.g.*, a polymer, an inorganic layer or a hybrid composite. For this purpose, forming an adhesive bond to joint two different materials plays an important role for the development of new devices or improvement of the well-known ones. The stability of the joints depends on the affinity between the coating and the substrate. One key factor for good adhesive bonding is starting from a clean, homogeneous and stable surface, and providing an appropriate roughness leads to an enlargement of the actual interface between the metal (oxide) surface and the adhesive as well as to securing sufficient wettability.[10] In order to achieve these requirements, several methodologies have been used, such as traditional wet-chemical acid/base etch treatment, electrochemical anodisation, plasma oxidation and laser treatments.[11] In the biomedical field, polydimethylsiloxane (PDMS) and polyurethane (PU) are polymeric materials used in implants, catheters, heart valves, due to their biocompatibility, low toxicity, thermal and chemical stability, among others. Thus, a PDMS-urethane (PDMSUr) based coating can be expected to provide combined characteristics of both the pristine PDMS and urethane material. In this work, a precursor cyclic(carbonate) PDMS-derived (CCPDMS), produced in previous work[12,13] was used, and terminated with an aminosilane, in order to form a difunctional non-isocyanate urethane as a base for a hybrid coating. Its properties are governed by silicate regions connected through urethane bonds. Aiming at improving the strength and durability of the adhesive bonding between the PDMSUr and metallic surfaces, the use of environmentally friendly low pressure plasma activation and pulsed Nd:YAG laser is proposed to modify Ti6Al4V and SS316L

Institute of Chemistry of São Carlos, University of São Paulo, 13563-120, São Carlos, SP, Brazil. E-mail: kelen.flores@gmail.com

bFraunhofer Institute for Manufacturing Technology and Advanced Materials IFAM, 28359, Bremen, Germany

cPontifical Catholic University of Rio Grande do Sul, 90619-900, Porto Alegre, RS, Brazil

dEngineering Faculty, State University Julio de Mesquita Filho, 15385-000, Ilha Solteira, SP, Brazil

surfaces by creating a rough oxide layer[14] ready to condensate with silanol moieties from the PDMSUr. The efficacy of the treatments on adhesion was established by performing Pull-off-tests and comparing activated substrates with non-activated substrates by low pressure plasma and laser. In addition, X-ray Photoelectron Spectroscopy (XPS) and optical microscopy were used to evaluate the features of the surfaces.

Experimental

Materials

Poly(dimethylsiloxane) diglycidyl ether terminated (**E-PDMS**, Sigma Aldrich), tetraethylammonium bromide (**TEAB**, 98%, Sigma Aldrich), carbon dioxide (99.99%, Linde gas), 3-amino-propyltriethoxysilane (**APTES**, >98%, Sigma Aldrich), 5-amino-1,3,3-trimethylciclohexano methylamine (**IPDA**, >99%, mixture of *cis/trans* isomers, Sigma Aldrich), 2-ethoxyethanol (EG, Sigma Aldrich), dimethylacetamide (**DMAc**, Sigma Aldrich), phospho-tungstic acid (**PWA**, Sigma Aldrich) dried at 60 °C overnight, commercially available titanium alloy Ti6Al4V (25 × 25 × 1 mm) and biomedical grade stainless steel SS316L (25 × 25 × 1 mm). Alkaline etching of the metallic substrates was performed using a solution (495 g L^{-1}, Henkel) of the commercial product Turco® 5578, which consists of sodium hydroxide, sodium metasilicate and sodium pyrophosphate.[15]

PDMSUr synthesis

Based on the experimental conditions proposed in the previous work published by our group[12] a PDMS-derived cyclic carbonate (CCPDMS) precursor was synthesized by carbon dioxide fixation into epoxy groups of the **E-PDMS**, in the presence of catalyst **TEAB**. The CCPDMS precursor was used to react with **APTES** and **IPDA**, applying the following procedure: 1 mmol of CCPDMS and 3 mmol of **APTES** (PDMSUr 1) were weighed in a glass vial and heated at 70 °C for 40 minutes under stirring. After this time, **PWA** (35% or 1 w/w%) previously dissolved in **DMAc** was added, and the mixture was allowed to stir for 24 h at 50 °C. The second composition of the hybrid adhesive (PDMSUr 2) was prepared by mixing 1 mmol of CCPDMS and 0.75 mmol of **IPDA** for 20 minutes at 70 °C. Afterwards, 2.25 mmol of **APTES** were added to the mixture, which was allowed to stir for 20 minutes more. After this time, **PWA** (35% or 1% w/w) dissolved in **DMAc** was added and the solution was stirred for 24 h at 50 °C. Scheme 1 depicts the fluxogram for PDMSUr synthesis.

Preparation of the specimens

SS316L and Ti6Al4V were etched in a Turco® 5578 solution for 10 minutes at 90 °C, as described by.[15] Afterwards, the samples were rinsed three times with deionized water at room temperature and dried with nitrogen steam. As soon as the etching process was finished, the substrates were treated by plasma or laser. On the treated surfaces, 500 μL of a PDMSUr solution (10% w/v) in **DMAc** were dropped on the metallic substrates. The specimens were placed on a hot plate during 1 h and afterwards in a vacuum oven for 24 h at 60 °C.
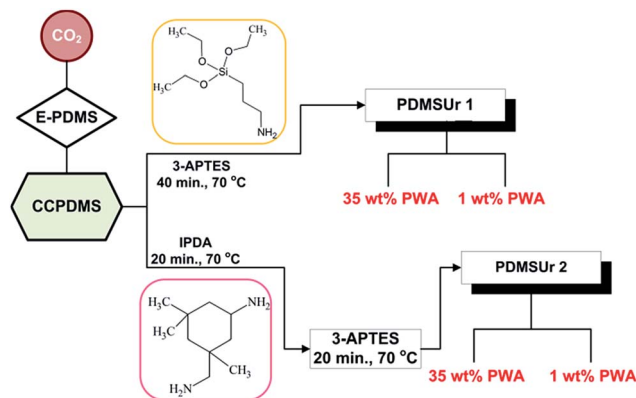
Scheme 1 Steps for the synthesis of polyhydroxyurethane PDMS derived (PDMSUr 1 and PDMSUr 2).

Pull-off-strength test

After the hardening of the hybrid coatings, an aluminum stud was fixed by using an epoxy resin bonded to the coating. The measurements were performed in five samples of each composition using an Elcometer 506 analogue and digital tester. Samples only etched by Turco® solution were used as control.

Plasma oxidation treatment

The substrates etched were placed inside the plasma chamber. The pressure was brought down to the desired low pressure (5.4 × 10^{-4} mbar). The plasma was turned on with argon (50 scc m^{-1}) during 120 s, after which the argon was released and the reactor was loaded with oxygen O_2 for 15 minutes in the activation stage at 600 V. Afterwards, the plasma was turned off and the reactor returned to atmospheric conditions upon introducing N_2. The coatings were applied very soon after the treatment.

Laser treatment

The samples were irradiated using a Q-switched CL 250 Nd:YAG (λ = 1064 nm) laser manufactured by Clean Lasersysteme GmbH. The system generates pulse frequencies in the range between 10 kHz and 40 kHz. In this study a pulse frequency of 10 kHz with pulse duration of 80 ns was used. The laser spot has a Gaussian shape with a full width at half maximum (FWHM) of 686 mm. The mean intensity during the pulse is 5.8 J cm^{-2} and the spot meanders across the surface with a line distance of 170 mm and a scan velocity of 1715 mm s^{-1}. Each repetition consists of a scan of parallel lines meandering on the surface of the sample and subsequently a scan perpendicular to the initial direction. The chosen laser parameters result in a processing rate of 1.5 cm^2 s^{-1} per scan or 0.7 cm^2 s^{-1} for the analysed single raster of the laser, respectively.

Contact angle measurements

Sessile drop method for contact angle determination of the surfaces coated by PDMSUr was applied and performed in an

OCA15 Plus (Data Physics Instruments, Germany) goniometer. The volume of the drops was kept in 10 μL for each measurement and the final contact angle was an average of three measurements in three different regions of the sample. The images were acquired with a CCD camera and the contact angle determined using the software SCAN 20 Data Physics.

Characterizations

Mid-infrared spectroscopy (FTMIR). A BOMEM MB102 FTIR spectrometer was employed to analyse the formation of the cyclic carbonate group and urethanic bonds in the range 250–4000 cm^{-1}, 32 scans and instrumental resolution set at 4 cm^{-1} in transmission mode (FTMIR-T) of analysis. The hybrid PDMSUr for FTIR analysis were prepared on silicon wafer by drop casting.

X-ray photoelectron spectroscopy (XPS). XPS spectra were taken using a Kratos Ultra system applying the following acquisition parameters: base pressure: 4×10^{-8} Pa, sample neutralisation applying low energy electrons (<5 eV), hybrid mode (electrostatic and magnetic lenses are used), take off angle of electrons 0°, pass energy 20 eV in high resolution spectra and 160 eV in survey spectra, excitation of photoelectrons by monochromatic AlKα radiation. The binding energy calibration was performed by referring the C 1s component of aliphatic carbon species to 285.0 eV and Shirley background.

Optical microscopy. Images of the metallic surfaces SS316L and Ti6Al4V were obtained by means of light microscopy using a Keyence VHX-600 digital light microscope. For topographical images, laser confocal microscope was applied using a Keyence model VK 9700. This model employs two sources of light: short wave laser and white light. The images were treated by correcting tilt and noise.

Solid nuclear magnetic resonance (NMR). Samples were cut into small pieces (<1 mm), dispersed in KBr and packaged in rotors (7 mm diameter) made of zirconia. The MAS rotation frequency was 5 kHz. Spectra of ^{29}Si were obtained by applying pulses of about 3.5 ms (π/2 pulses) with a delay time of 100 s, NS = 800. The chemical shift of ^{29}Si was referenced to TMS, using solid samples of kaolin.

Corrosion. The corrosion measurements were performed at room temperature in a conventional three electrode cell containing a platinum counter electrode (CE) and a saturated calomel electrode (SCE) as the reference electrode. The working electrode was Ti6Al4V coated with PDMSUr or uncoated, in the form of a square (5 cm^2). The substrates to be analysed were coated with 500 μL of PDMSUr and let to dry in a heater for 1 h and then placed in a vacuum oven for 24 h at 60 °C. The working surface area was 0.5 cm^2 and the electrochemical parameters E_{corr} (corrosion potential) and I_{curr} (current density) were obtained using the General Purpose Electrochemical System software (GPES 4.9). The potential was scanned with a speed of 1 mV s^{-1} over a range between −1.0 V and 1.2 V, controlled by a potentiostat PGSTAT 302 (Autolab). The corrosion behaviour of PDMSUr 1_35% and PDMSUr 2_35% on Ti6Al4V were analysed in Hank's solution. Hank's solution is a solution made at physiological pH and it includes sodium, potassium, calcium, magnesium and chloride.

Results and discussion

The hybrid polyhydroxyurethanes PDMS-derived (PDMSUr) are materials which contain on its chemical backbone polydimethylsiloxane segments, and as end group, silicate or ORMOSIL (Organically Modified Silica) regions. In case of PDMSUr 2, isophorone diamine (**IPDA**) was incorporated between PDMS and Ormosil segments as chain extender. Fig. 1 shows the proposed chemical structure for the hybrid PDMSUr's.

Cyclic carbonates, such as the precursor here prepared (CCPDMS), can react with several nucleophiles. The most explored reaction of cyclic carbonate it is been the aminolysis *via* Ring Opening Polymerization (ROP), which consists of the nucleophilic addition of amines into cyclic carbonate functional group.[16] According to Fig. 2, the beginning of the reaction comprehends the nucleophilic attack into the carbonyl carbon of the cyclic carbonate followed by the cleavage of the C–O bond and the formation of a reactive specie – an alcoholate.[17] When the five membered cyclic carbonate reacts with an amino compound, the generated product is a β-hydroxyurethane, it
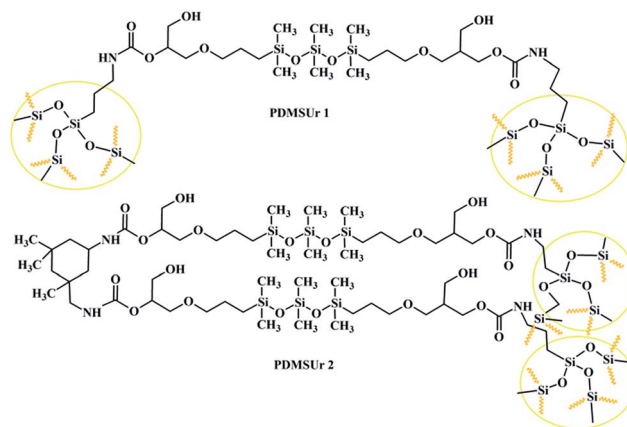

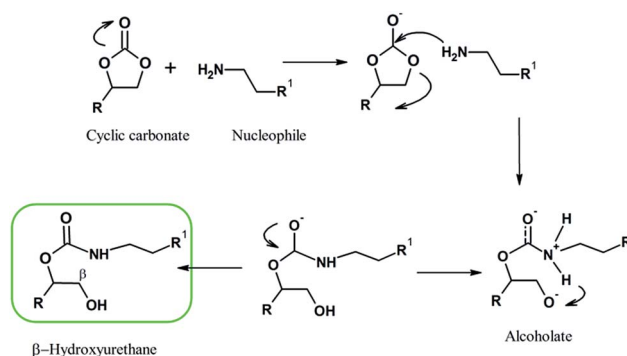Fig. 1 Chemical structure of the PDMSUr hybrid system. The yellow circles represent the ormosil regions.

Fig. 2 Ring Opening Polymerization (ROP) mechanism.

means, the chain will contain a hydroxyl group at the β position in relation to the urethane bond.[18]

Regarding the synthesis of the hybrid urethane coatings, Fig. 3A shows superimposed FTIR spectra of the urethanes PDMSUr 1, PDMSUr 2 and the precursor CCPDMS. The black dashed lines show the wavenumber position for vibrations of the common urethane linkages and the arrow indicates the carbonyl band $\nu_{C=O}$ from the precursor CCPDMS, which is placed at around 1800 cm^{-1}.[12,19] At 1537 cm^{-1} there is a characteristic peak of the urethane linkage (N–H bond)[20] and a second one in the region between 1700 and 1730 cm^{-1}, that corresponds to self-associated urethane by hydrogen bond (H-bond) or to free urethane.[21] The indication of the formation of urethanic hybrid material is given by the disappearance of the carbonyl band ($\nu_{C=O}$) from CCPDMS. The PDMS segment is characterised by the presence of a doublet between 1100 cm^{-1} and 1020 cm^{-1}, correspondent to symmetric and asymmetric stretching of the siloxane bonds Si–O–Si (ν_{as} and ν_s, respectively).[22] The condensation of silanol groups in sol–gel process allows the formation of silicate regions which are a host network for polyoxometalates, such as phosphotungstic acid. **PWA** acts as a catalyst in the hydrolysis and condensation reactions, besides providing other properties to the material,

such as electrical[23] and mechanical[24] functionalities. The FTIR spectrum of PDMSUr 1_35 wt% **PWA** is shown in Fig. 3B. The hybrid film showed absorption bands characteristic of the Keggin structure of **PWA**, indicating the preservation of the molecules inside the films. The corresponding peaks of **PWA** are detected at 1080 cm^{-1} [P–O$_a$], 984 cm^{-1} [W=O$_d$], 889 cm^{-1} [ν_{as}(W–O$_b$–W)], and 802 cm^{-1} [ν_s(W–O$_c$–W)].[23,25]

More detailed inspection of the vibrational bands revealed that the band related to the W=O$_d$ bond ($\Delta\nu \sim 9$ cm^{-1}) inside the hybrid urethane matrix is shifted to lower wavenumbers, *i.e.* to the red region of the electromagnetic spectrum (from 984 cm^{-1} to 976 cm^{-1}). A slightly smaller shift is observed for the band of ν(P–O$_a$) (from 1080 cm^{-1} to 1075 cm^{-1}). On the other hand, the ν_{as}(W–O$_b$–W) absorption has shifted to the blue region of the electromagnetic spectrum (from 889 cm^{-1} to 895 cm^{-1}). This finding can indicate interactions between Keggin ions and silicate regions, mainly silanol groups, and columbic interactions between the organic matrix and the hetero-polyanion.[26] These findings were reported in previous work, as well as the ^{29}Si Nuclear Magnetic Resonance (NMR) in solid state of the hybrid films.[27] Here, in Fig. 4, we reproduce the ^{29}Si NMR spectra of PDMSUr 1 and PDMSUr 2 showing the formation of the tridimensional ORMOSIL regions which are mainly anchored by T$_3$ structures.

As observed in Fig. 4, a signal around −68 ppm indicates the presence of T$_3$ structure where the silicon atom is binding three siloxane bonds (Si–O). This sort of structure is expected for a trialkoxysilane.[28,29] The resonance signal at −22.3 ppm is related to the non-hydrolysable silicon atoms D (O–Si–(CH$_3$)$_2$–O) from the PDMS segment.[30] Around 7.6 ppm, the resonance from the second silicon atom M (–Si(CH$_3$)$_2$–CH$_2$–) from the PDMS chain is observed.

Optical microscopy was employed to visualize changes on the surface of Ti6Al4V and SS316L after the physical treatments. Samples prior and after laser or plasma treatment showed, in
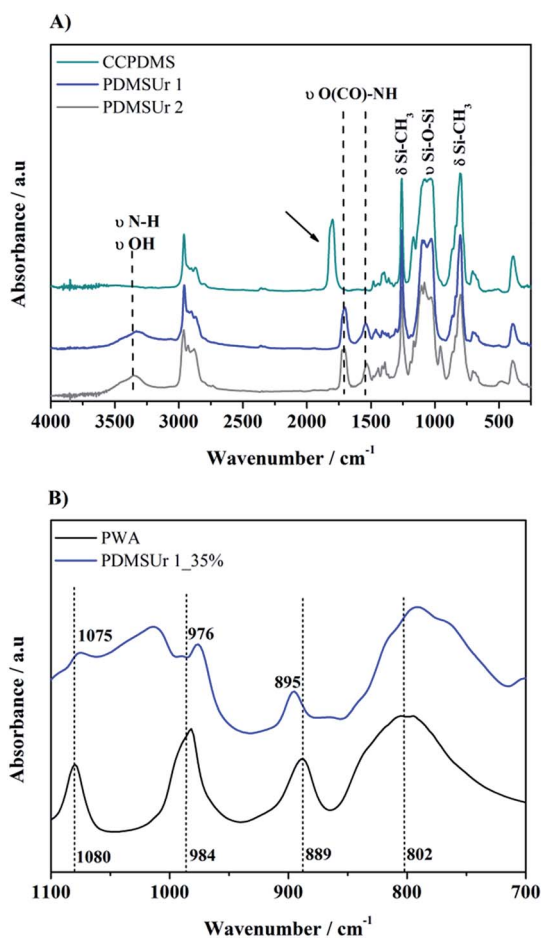

Fig. 3 Infrared spectra of hybrid PDMSUr 1, PDMSUr 2, and CCPDMS (A) and zoomed spectra of PDMSUr 1_35% **PWA** and pristine **PWA** (B).
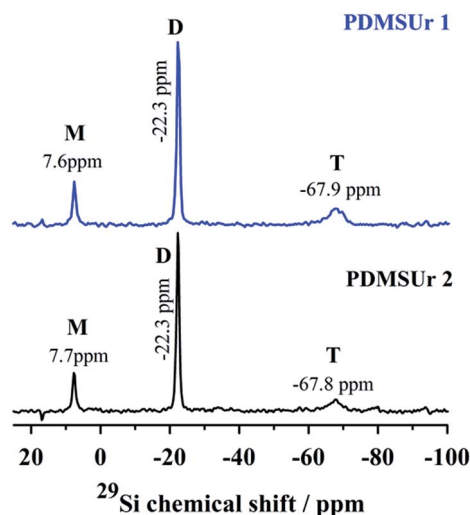

Fig. 4 ^{29}Si NMR spectra of PDMSUr 1 and PDMSUr 2 in the solid state. The peaks correspondent to structures M, D and T are observed at its typical chemical shifts.

a macroscopic scale, changes in the absorption and reflection behaviour of the light, as shown in Fig. 5.

A notable change in the gray colour to light brown colour was observed on the substrates after plasma activation; for laser treated samples, aligned grooves were noticed, that could be related to heat-induced modifications of the outermost surface.[10] In previous works it was shown, that multiple laser treatments resulted in a clean and – in case of Ti6Al4V – in a nano-structured surface layer with high surface enlargement.[10] These surfaces appear ideal for durable adhesive joining, because of the formation of a nano-composite interlayer permitting an infiltration of the adhesive into the nano porous oxide layer obtained after laser treatment.[31] Fig. 6 shows confocal microscopy images of the substrates Ti6Al4V and SS316L after and before irradiation with laser, and the topographical profile of the metallic surfaces is also shown.

The impact of laser irradiation is expected to be associated with changes in topography, morphology and composition of the surface. The image of the SS316L substrate suggests pores on the surface which were not observed on the surface before treatment. In the case of Ti6Al4V surface, the formation of surface microcracks after laser treatment is observed (Fig. 6D). This feature is most likely induced by high temperature gradients and superficial oxidation processes due to switching on and off the laser beam in air.[10] For the SS316L, the topographical profile height deviations from the mean line (R_q) changed from 0.138 μm to 0.323 μm after the physical treatment, with the surface getting rougher. In contrast, for the titanium alloy surface, the R_q value decreased from 0.501 mm to 0.281 mm which indicates a more homogeneous oxide layer formation on top.

With respect to surface composition, Fig. 7 shows the Ti 2p and Fe 2p core level spectra of SS316L and Ti6Al4V treated by laser. The surface investigation reveals peaks from the oxide
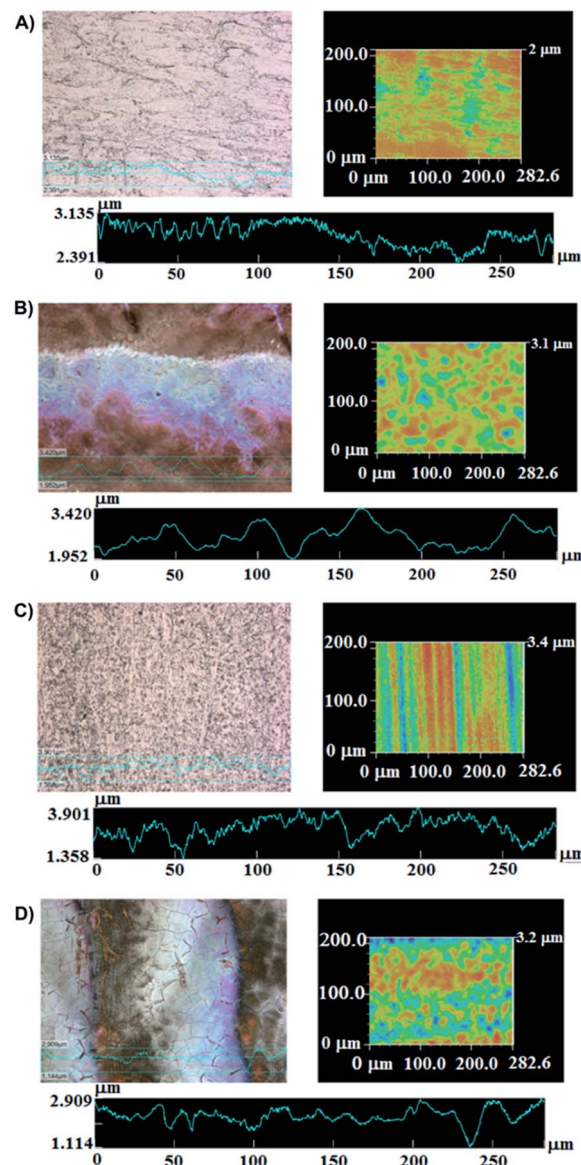

Fig. 6 Microscopic images of SS316L substrate before (A) and after (B) treatment by laser irradiation. Images (C) and (D) correspond to Ti6Al4V untreated (C) and treated (D) by laser. Images were taken with 50 fold amplification and the dimensions are given in micrometers.
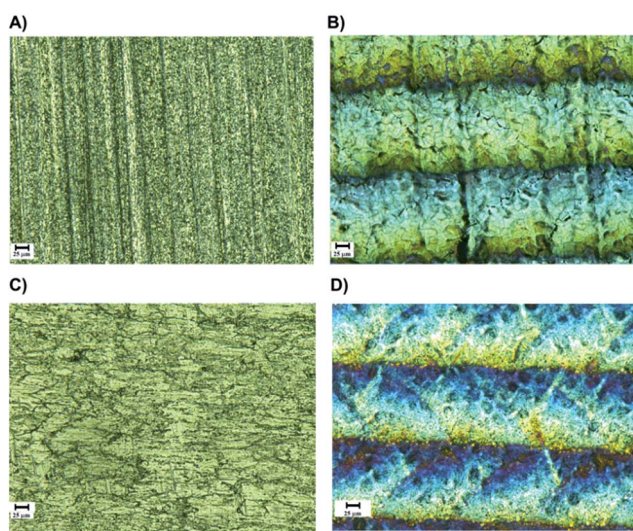

Fig. 5 Optical microscopies of the surfaces of Ti6Al4V untreated (A) and Ti6Al4V laser treated (B); SS316L untreated (C) and SS316L laser treated (D). The images were taken with amplification of 500 times and the scale bar corresponds to 25 μm.

layer, characterized by the Fe $2p_{3/2}$ signal at 711 eV, Fe $2p_{1/2}$ at 724 eV and a shake-up peak at 719 eV (ref. 32 and 33) consistent with the presence of Fe_2O_3 on SS316L. The binding energy of about 708 eV for the Fe $2p_{3/2}$ peak is related to metallic state Fe^0. For the titanium alloy surface, after treatment by laser, the Ti 2p doublet consisted of Ti $2p_{3/2}$ at 458.5 eV, characteristic of a Ti^{4+} state in a TiO_2 neighbourhood, and Ti $2p_{1/2}$ at 464.2 eV (ref. 10 and 34) which is consistent with the presence of TiO_2 contributing to the topmost layer composition. On the other hand, also the Ti6Al4V surface treated by plasma presented mainly peaks at 458.5 eV and 464.1 eV, assigned to a TiO_2 layer. However, the titanium surface treated by plasma still showed a Ti $2p_{3/2}$ peak at 453.5 eV (ref. 29) attributed to Ti^0 and, as well, signal characteristic for species Ti^x.[10] As compared to the surface state
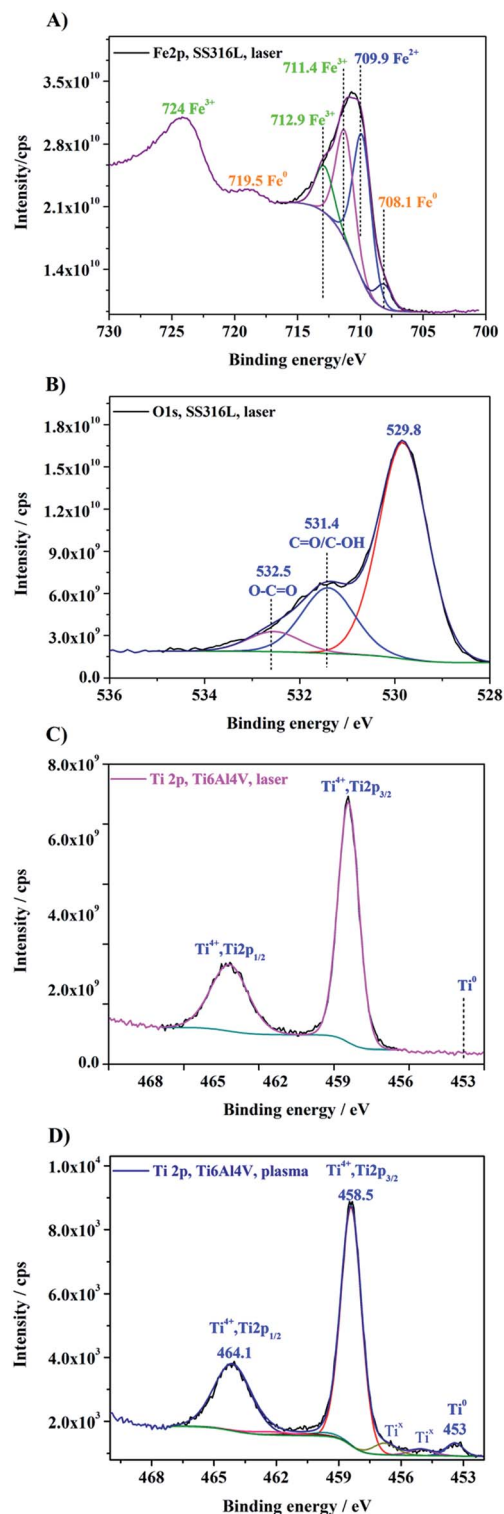
Fig. 7 XPS core level spectra of Fe 2p (A) and O 1s (B) for a laser treated SS316L and core level spectra of Ti 2p signals for Ti6Al4V surfaces after laser (C) and plasma treatment (D).

before treatment, the latter signals were clearly less intense, which indicates a thickness of the oxide layer below 10 nm. The O 1s binding energy for the oxide species in the TiO_2 layer was found at 530.3 eV and for the Fe_2O_3 at 529.8 eV (Fig. 7B), in

accordance with assigning an O 1s binding energy of 530 eV to oxygen atoms in the iron oxide.[32] The other oxygen-containing groups, observed in Fig. 7B for the laser treated SS316L surface, are interpreted to be from $C=O^*/C-O^*H$ at around 531.4 eV and sulphates or $O-C=O^*$ at 532.3 eV.[35]

The influence of laser treatment on the results obtained in the pull-off-test is evidenced in Fig. 8. The average value and standard deviation of the adhesion strength were calculated for a series of five samples for each composition (PDMSUr 1_35% **PWA**, PDMSUr 1_1% **PWA**, PDMSUr 2_35% **PWA** and PDMSUr 2_1% **PWA**). Based on the findings displayed in Fig. 8, an increase in the pull-off-strength by 128% and 146% for steel SS316L and Ti6Al4V, respectively, was noticed for the coatings prepared with PDMSUr1_35% **PWA**. Coatings prepared with PDMSUr 2_35% **PWA** on SS316L showed pull-off-strength values increased by 46% as compared to joints comprising etched adherents. The other compositions did not show significant changes on adhesion. Among the coatings investigated, the outstanding results obtained for PDMSUr 1_35% **PWA** may be discussed referring to its chemical composition characterized by the higher amounts of **APTES** and the catalyst phospho-tungstic acid. According to previous work from our group, **PWA** and **APTES** are capable to increase the hardness and elastic modulus of the urethane hybrid films in at least five times;[27] this means that a more rigid film is obtained when the density of silicate regions is favoured by the crosslinking[36] of available alkoxy groups in the layer-forming urethane. Lakshminarayana and Nogami observed an improvement on the mechanical properties of Nafion® after the addition of **PWA**.[37]

Both characteristics, topographical changes on the substrates and chemical characteristics of the coatings might have contributed to the pull-off-strength behaviour observed in Fig. 8. For both substrates, the oxide layer formation and the topography created by laser treatment were suitable for the improvement of the pull-off strength of PDMSUr on the substrates. Changes in the surface topography and sample morphology of the titanium or steel surfaces were observed by optical microscopy. Accordingly, the bonding formation between silicate regions and the metal oxide top layer (Si–O–M) played an important role in the stabilization of the coating on metallic surfaces. Finally, coatings made of PDMSUr 1_35% **PWA** were prepared on SS316L and Ti6Al4V in order to test the adhesion strength after plasma treatment on the surfaces. Fig. 9 shows the results of pull-off-test of PDMSUr 1 containing 35% of phosphotungstic acid. The adhesion of PDMSUr 1_35% **PWA** increased around 177% on titanium alloy and around 139% on steel after plasma treatment. Different types of (contributions to) fracture images (adhesive, cohesive and mixed fracture) were observed in the samples after detachment of the coating by pull-off-test.

The corrosion resistance of metallic substrates used in dental or orthopaedic implants is very important issue in the biomaterials field. These biomedical grade metallic implants, such as titanium and its alloys, are in incessant contact with the physiological fluid, which is rich in ions chloride able to promote the oxidation of the metal. In the oral cavity, for instance, occurs galvanic corrosion.[38] Thus, in order to evaluate
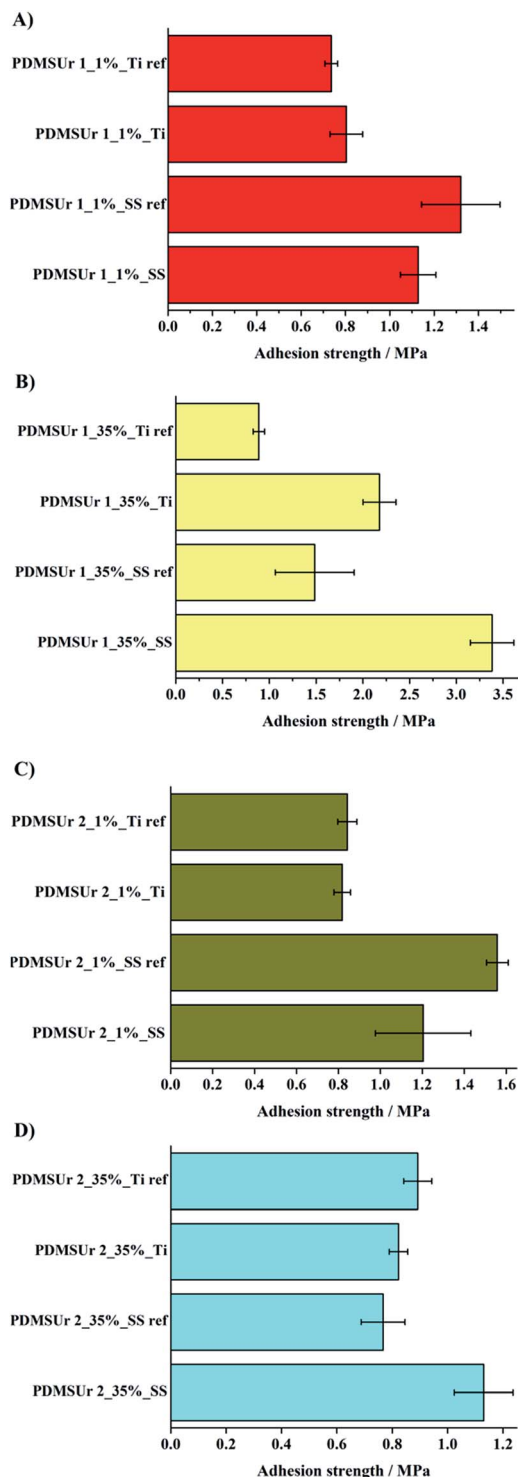
Fig. 8 Pull-off-test results of the hybrid coatings: (A) PDMSUr 1_1% **PWA** on SS316L and Ti6Al4V; (B) PDMSUr 1_35% **PWA** on SS316L and Ti6Al4V; (C) PDMSUr 2_1% **PWA** on SS316L and Ti6Al4V and (D) PDMSUr 2_35% **PWA** on Ti6Al4V and SS316L substrates treated by laser. Ti ref and SS ref correspond to the substrates only etched by Turco®.

Fig. 9 Pull-off-strength of PDMSUr 1_35% **PWA** coating on SS316L and titanium alloy after plasma treatment. The metallic substrates without any treatment were used as control.

Table 1 E_{corr} and J_{corr} presented by the samples PDMSUr 1_35%, PDMSUr 2_35% and, Ti6Al4V bare substrate tested in Hank's solution

	Ti6Al4V	PDMSUr 1_35%	PDMSUr 2_35%
E_{corr}	−0.42 V	−0.49 V	−0.32 V
J_{corr}	1.68×10^{-6} A cm^{-2}	2.29×10^{-8} A cm^{-2}	2.95×10^{-7} A cm^{-2}

density (J_{corr}) values taken from the corresponding Tafel's curves of Fig. 10.

According to the potentiodynamic polarization curves or Tafel's curves in Fig. 10, which were obtained from the hybrid PDMSUr 1_35% and PDMSUr 2_35% coatings on Ti6Al4V, the corrosion potential (E_{corr}) or the intersection point of the individual cathodic and the anodic plots did not changed significantly when compared with the bare Ti6Al4V substrate. However, when the current density (J_{corr}) is analysed, lower values were presented by the metallic substrate coated with

the behaviour of the hybrid films in physiological medium, experiments of corrosion were performed in Hanks solution. Table 1 comprises the corrosion potential (E_{corr}) and current
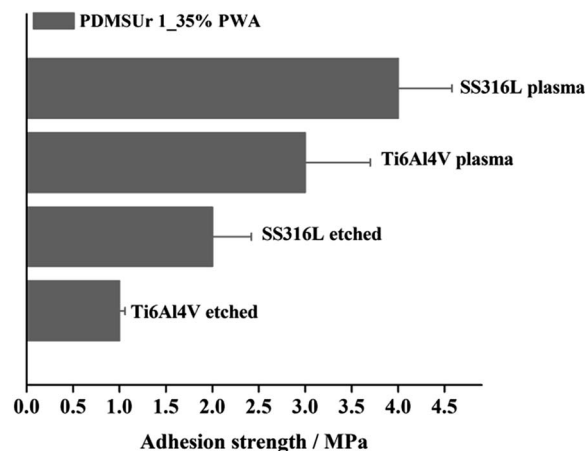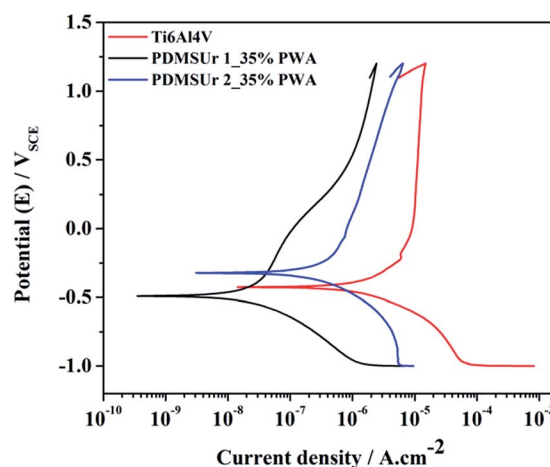

Fig. 10 Representative potentiodynamic curves obtained from samples PDMSUr 1 and 2 containing 35% of **PWA** in Hanks solution and bare substrate Ti6Al4V.

Table 2 Contact angles of PDMSUr 1_1%, PDMSUr 1_35%, PDMSUr 2_1% and PDMSUr 2_35%, measured by sessile drop

Sample	Contact angle (°)
PDMSUr 1_1% **PWA**	104.7 ± 0.2
PDMSUr 1_35% **PWA**	104.3 ± 0.4
PDMSUr 2_1% **PWA**	102.8 ± 0.3
PDMSUr 2_35% **PWA**	103.3 ± 0.2

hybrid PDMS urethanes. The polymeric layer prevents somehow the diffusion of oxidative species such as H^+, oxygen and even water from the aqueous medium to the metallic surface. This behaviour leads to a lower current density, since the availability of the components responsible for the oxidation may have been reduced. Thus, both PDMSUr were suitable anti-corrosive coatings for Ti6Al4V in physiological solution acting as a physical barrier against corrosion.

Another important feature to prevent corrosion is the hydrophobicity of the protective.[39] The synthesized PDMSUr presented hydrophobic surfaces with high contact angle, as shown in Table 2. The contact angles were about 102–104° close to the polydimethylsiloxane (PDMS) contact angle which is around 95–110°.[40,41] The hydrophobicity is inherent to the PDMS segments. The amounts of **PWA** used in the compositions did not affect the contact angle or the characteristics of the surface, indicating a repeatability of surface among the samples.

Conclusions

Polydimethylsiloxane hybrid urethane (PDMSUr) coatings were successfully synthesized by ring opening polymerization of a precursor bis(cyclic carbonate) PDMS derived (CCPDMS). The hybrid coatings presented ormosil regions anchored by tridimensional structures (T_3) formed by condensation of silanol into siloxane bonds. By drop casting, the PDMSUr were deposited on a treated biomedical grade metallic surfaces, such as Ti6Al4V and SS316L, in order to form a coating. The physical treatment for surface modification consisted in oxygen plasma and laser. The treated surfaces presented an oxide layer (Fe_2O_3 or TiO_2) on the top according the XPS results. Such sustainable surface pre-treatment was the base for bonding of hybrid PDMS-urethane coatings. This finding was confirmed by pull-off-strength measurements which showed significant increment in the adhesion of the coatings of more than 100%, when compared with the biomedical grade metals stainless steel and titanium alloy untreated. The hybrid coatings are good candidates for coating metallic surfaces used for orthopaedic or dental implants presenting desirable adhesion strength (1 to 4 MPa). In addition, they may contribute in avoiding the corrosion of the metal when in contact with physiological medium by means of a hydrophobic physical barrier.

Acknowledgements

References

1 N. Adya, M. Alam, T. Ravindranath, A. Mubeen and B. Saluja, *Journal of Indian Prosthodontic Society*, 2005, **5**, 126.

2 K. T. Oh, S. U. Choo, K. M. Kim and K. N. Kim, *Eur. J. Orthod.*, 2005, **27**, 237.

3 C. C. Gomes, L. M. Moreira, V. J. S. V. Santos, A. S. Ramos, J. P. Lyon, C. P. Soares and F. V. Santos, *Genet. Mol. Biol.*, 2011, **34**, 116.

4 A. Choubey, B. Basu and R. Balasubramaniam, *Trends Biomater. Artif. Organs*, 2005, **18**, 64.

5 J. B. Park and R. S. Lakes, *Biomaterials: An introduction*, Springer, New York, 3rd edn, 2007.

6 P. Schmutz, N. C. Quach-Vu and I. Gerber, *Electrochem. Soc. Interface*, 2008, **17**, 3.

7 Y. Okazaki and E. Nishimura, *Mater. Trans.*, 2000, **41**, 1246.

8 D. Cadosch, E. Chan, O. P. Gautschi and L. Filgueira, *J. Biomed. Mater. Res., Part A*, 2009, **91**, 1252.

9 S. Torgersen and N. R. Gjerdet, *J. Mater. Sci.: Mater. Med.*, 1994, **5**, 256.

10 S. Zimmermann, U. Specht, L. Spieß, H. Romanus, S. Krischok and M. Himmerlich, *J. Mater. Sci. Eng. A*, 2012, **558**, 755.

11 P. Molitor, V. Barron and T. Young, *Int. J. Adhes. Adhes.*, 2001, **21**, 129.

12 K. R. Aguiar, V. Santos, M. N. Eberlin, K. Rischka, M. Noeske, G. Tremiliosi-Filho and U. P. Rodrigues-Filho, *RSC Adv.*, 2014, **4**, 24334.

13 V. Carrillo Beber, L. T. Caleiro, K. R. Aguiar, J. O. Joswig, U. P. Rodrigues-Filho, P. L. M. Noeske, K. Rischka and W. Leite Cavalcanti, *Appl. Adhes. Sci.*, 2015, **3**, 2.

14 R. A. DiFelice, PhD thesis, Virginia Polytechnic Institute, Virginia, 2001.

15 G. W. Critchlow and D. M Brewis, *Int. J. Adhes. Adhes.*, 1995, **15**, 161.

16 B. Nohra, L. Candy, J. F. Blanco, Y. Raoul and Z. J. Mouloungui, *J. Am. Oil Chem. Soc.*, 2012, **89**, 1125.

17 T. Endo, *General mechanisms in ring-opening polymerization*, Wiley-VCH, Weinheim, Germany, 2009.

18 E. Pretsch, P. Bühlmann and M. Badertscher, *Structure Determination of Organic Compounds*, Springer, Heidelberg, Germany, 2009.

19 J. Van Holen, Process using a cyclic carbonate reactant and beta-hydroxyurethanes thereby obtained, *US Pat.*, US20040236119, November 25 2004.

20 S. A. E. All, *J. Phys. D: Appl. Phys.*, 2007, **40**, 6014.

21 L. Ning, W. D. Ning and Y. Sheng-Kang, *Macromolecules*, 1997, **30**, 4405.

22 J. N. Chazalviel and U. P. Rodrigues-Filho, *Thin Solid Films*, 2012, **520**, 391.

23 U. L. Štangar, N. Grošelj, B. Orel and P. Colomban, *Chem. Mater.*, 2000, **12**, 3745.

24 I. Al-Namie, A. A. Ibrahim and M. F. Hassan, *Iraqi J. Mech. Mater. Eng.*, 2011, **11**, 486.

25 S. Ullah, A. J. J. Sáez, A. A. Pasa, S. A. Bilmes, M. E. Vela, G. Benitez and U. P. Rodrigues-Filho, *Appl. Surf. Sci.*, 2013, **277**, 111.

26 M. Hasik, A. Pron, J. Poźniczek, A. Bielański, Z. Piwowarska, K. Kruczala and R. Dziembaj, *Faraday Trans.*, 1994, **90**, 2099.

27 K. M. F. Rossi de Aguiar, E. P. Ferreira-Neto, S. Blunk, J. F. Schneider, C. A. Picon, C. M. Lepienski, K. Rischka and U. P. Rodrigues-Filho, *RSC Adv.*, 2016, **6**, 19160.

28 F. Bauer, H. J. Glasel, E. Hartmann, E. Bilz and R. Mehnert, *Nucl. Instrum. Methods Phys. Res., Sect. B*, 2003, **208**, 267.

29 Z. L. Da, *eXPRESS Polym. Lett.*, 2007, **1**, 698.

30 F. Joki-Korpela and T. T. Pakkanen, *Eur. Polym. J.*, 2011, **47**, 1694.

31 U. Specht, J. Ihde and B. Mayer, *Materialwiss. Werkstofftech.*, 2014, **45**, 1116.

32 T. Fujii, F. M. F. Groot and G. A. Sawatzky, *Phys. Rev. B: Condens. Matter*, 1999, **59**, 3195.

33 Y. Matsumoto, *J. Solid State Chem.*, 1996, **126**, 227.

34 M. Müller, X. Zhang, Y. Wang and R. A. Fischer, *Chem. Commun.*, 2009, 119.

35 M. Radecka, *Thin Solid Films*, 2004, **98**, 451.

36 A. M. Grillet, N. B. Wyatt, L. M. Gloe and H. Tai, *Polymer Gel Rheology and Adhesion*, ed. J. De Vicente, INTECH, Livermore, 2012, p. 350.

37 G. Lakshminarayana and M. Nogami, *J. Phys. Chem. C*, 2009, **113**, 14540.

38 I. Patrascu, V. G. Vasilescu and S. Milicescu, *InTech*, 2014, 171.

39 T. Ishizaki, I. Shigematsu and N. Saito, *Surf. Coat. Technol.*, 2009, **203**, 2288.

40 R. A. Lawton, C. R. Price, A. F. Runge, W. J. Doherty and S. S. Saavedra, *Colloids Surf., A*, 2005, **253**, 213.

41 M. K. Chaudhury, *J. Adhes. Sci. Technol.*, 1993, **7**, 669.